C2012-0001321

NACE INTERNATIONAL CORROSION 2012 CONFERENCE & EXPO

Mechanistic Modeling of Carbon Steel Corrosion in a MDEA-Based CO_2 Capture Process

Yoon-Seok Choi
Institute for Corrosion and Multiphase Technology, Department of Chemical and Biomolecular Engineering, Ohio University
342 West State Street
Athens, OH, 45701
USA

Srdjan Nešić
Institute for Corrosion and Multiphase Technology, Department of Chemical and Biomolecular Engineering, Ohio University
342 West State Street
Athens, OH, 45701
USA

Deli Duan
Institute of Metal Research, Chinese Academy of Sciences
72 Wenhua Road
Shenyang, 110016
China

Shengli Jiang
Institute of Metal Research, Chinese Academy of Sciences
72 Wenhua Road
Shenyang, 110016
China

ABSTRACT

A predictive model was developed for corrosion of carbon steel in CO_2-loaded aqueous methyldiethanolamine (MDEA) systems, based on modeling of thermodynamic equilibria and electrochemical reactions. The concentrations of aqueous carbonic and amine species (CO_2, HCO_3^-, CO_3^{2-}, MDEA and $MDEAH^+$) as well as pH values in the MDEA solution were calculated. The water chemistry model showed a good agreement with experimental data for pH and CO_2 loading, with an improved correlation upon use of activity coefficients. The electrochemical corrosion model was developed by modeling polarization curves based on the given species concentrations. The required electrochemical parameters (e.g., exchange current densities, Tafel slopes and reaction orders) for different reactions were determined from experiments conducted in glass cells. Iron (Fe) oxidative dissolution, bicarbonate (HCO_3^-) reduction and protonated alkanolamine ($MDEAH^+$) reduction reactions were implemented to build a comprehensive model for corrosion of carbon steel in an MDEA-CO_2-H_2O environments. The model is applicable to uniform corrosion when no protective films are present. A solid foundation is provided for corrosion model development for other amine-based CO_2 capture processes.

Key words: MDEA, corrosion model, CO_2 capture, carbon steel, carbon capture and storage

INTRODUCTION

Amine-based CO_2 capture process has gained more interest recently as the immediate technological solution that can be used for capturing CO_2 from flue gas streams emitted from coal-fired power plant.[1,2]

Although amine-based CO_2 capture process has been proven in current industrial processes such as natural gas production, syngas scrubbing, etc., the amine process is associated with several technical challenges.[3] One of the major problems is corrosion of process components which results in unexpected downtime, production loss and even fatalities.
Corrosiveness of an amine solution after CO_2 absorption depends on the type and concentration of amine, CO_2 loading, temperature, solution turbulence, etc.[4] From a corrosion standpoint, methyldiethanolamine (MDEA, $CH_3N(C_2H_4OH)_2$) is the most "forgiving" alkanolamine because it is a tertiary amine and it does not form carbamate (R_3NCOO^-) with CO_2.[5-7] Although there are extensive research data available on corrosion and corrosion inhibition in amine-CO_2 systems,[8-12] minimal information has been reported in the literature which could aid in establishing a corrosion model for carbon steel in such systems. Veawab and Aroonwilas[13] reported a mechanistic corrosion model to identify the oxidizing agents responsible for corrosion reactions in the monoethanolamine (MEA, $(CH_2)_2OHNH_2$) system. Results indicated that bicarbonate ion and water are the primary oxidizing agents and hydrogen ion played an insignificant role in the reduction reaction.

The objective of the present study was to develop a predictive model for corrosion of carbon steel under operating conditions in the absorber with MDEA related to the CO_2 capture process in fossil fuel-fired power plants.

SPECIATION MODEL FOR AN MDEA/CO_2/H_2O SYSTEM

Thermodynamic framework

When CO_2 is dissolved and reacted with the MDEA, one can identify eight main species in the solution (MDEA, H_2O, CO_2(aq), $MDEAH^+$, HCO_3^-, CO_3^{2-}, H_3O^+, and OH^-). Carbonic acid (H_2CO_3) is not included here as it has a much lower concentration compared to other carbonic species (HCO_3^- and CO_3^{2-}), and the activity coefficient data for this species were not available in the open literature. Furthermore, in the follow-up electrochemical work it was confirmed that this H_2CO_3 does not contribute much to the overall corrosion process and could be omitted from the analysis. The following chemical reactions were considered:

$$CO_2\,(g) \xleftrightarrow{K_1} CO_2 \quad (1)$$

$$CO_2 + 2H_2O \xleftrightarrow{K_2} HCO_3^- + H_3O^+ \quad (2)$$

$$HCO_3^- + H_2O \xleftrightarrow{K_3} CO_3^{2-} + H_3O^+ \quad (3)$$

$$MDEAH^+ + H_2O \xleftrightarrow{K_4} MDEA + H_3O^+ \quad (4)$$

$$2H_2O \xleftrightarrow{K_5} OH^- + H_3O^+ \quad (5)$$

The reactions shown above can be described by equilibria reactions which can be solved by using the known values of the equilibrium constants (K), to obtain the concentrations of species (c_i). The equilibrium constants are a function of the temperature and are available in the open literature:[14,15]

$$K_1 = \frac{c_{CO_2}}{pCO_2} \quad (6)$$

$$K_2 = \frac{c_{HCO_3^-} c_{H_3O^+}}{c_{CO_2} c_{H_2O}^2} \quad (7)$$

$$K_3 = \frac{c_{CO_3^{2-}} c_{H_3O^+}}{c_{HCO_3^-} c_{H_2O}} \quad (8)$$

$$K_4 = \frac{c_{MDEA} c_{H_3O^+}}{c_{MDEAH^+} c_{H_2O}} \quad (9)$$

$$K_5 = \frac{c_{OH^-} c_{H_3O^+}}{c_{H_2O}^2} \quad (10)$$

where pCO_2 is the partial pressure of CO_2.

Since the solution cannot have a net charge, an electroneutrality equation is:

$$c_{MDEAH^+} + c_{H_3O^+} = c_{HCO_3^-} + 2c_{CO_3^{2-}} + c_{OH^-} \quad (11)$$

In addition, a mass balance can be written for MDEA and carbonic species in the solution:

$$c_{MDEA} + c_{MDEAH^+} = \text{constant} \quad (12)$$

$$c_{CO_2} + c_{HCO_3^-} + c_{CO_3^{2-}} = \text{constant} \quad (13)$$

The "constants" in the two mass balance equations above depend on the given concentration of MDEA and CO_2 loading in the aqueous solution, respectively. The concentrations of all species can be calculated by solving above eight equations (6) - (13).

Calculation of activity coefficients

In order to account for the non-ideality of the solution, in the present study, the Deshmukh-Mather model is used to evaluate activity coefficient for the species in the MDEA/CO_2/H_2O solution:[16]

$$\ln\gamma_i = -\frac{AZ_i^2\sqrt{I}}{1+B\sqrt{I}} + 2\sum\beta_{i,j}c_i \quad (14)$$

where γ_i is the activity coefficient for species i in the solution used to correct the concentration of species c_i. The first term on the rhs is based on Debye-Huckel theory, which accounts for the contribution due to the electrostatic forces among all ions in solution. Z_i is the electrical charge of ion i; B equals to 1.2; I is the ionic strength of the solution and A is taken as a function of temperature as proposed by Lewis et al.[17] The second term on the rhs expresses the contribution from short-range interaction forces among species in the solution. β_{ij} are the interaction parameters between the different species i and j in the solution.

Verification: Comparison with experiments

In order to verify the speciation model, CO_2 loading and pH measurements were conducted at different CO_2 partial pressures from 0.05 bar to 1.0 bar. The work was carried out in a 2L glass cell with 50 wt.% MDEA at 50°C. The CO_2 loading was measured by the methanoic KOH titration method. The pH electrode and meter were calibrated at the testing temperature (50°C) with pH 7 and 10 buffer solutions.

CORROSION MODEL FOR CARBON STEEL IN AN MDEA/CO_2/H_2O SYSTEM

The corrosion model was based on describing the electrochemical process taking place at the steel surface exposed to an MDEA/CO_2/H_2O environment, as schematically illustrated in Figure 1.

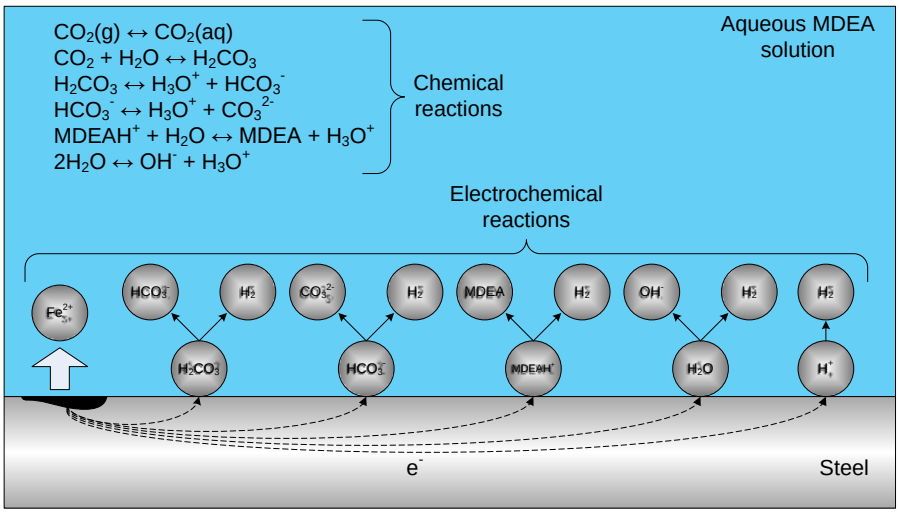

Figure 1: Schematic of corrosion process in MDEA-CO_2-H_2O environments

Electrochemical reactions at the steel surface

As shown in Figure 1, the electrochemical reactions occurring simultaneously at the steel surface are dissolution of iron and reduction of the various "oxidizing agents":

- Anodic (oxidation) reaction
  - $Fe \rightarrow Fe^{2+} + 2e^-$ (15)
- Cathodic (reduction) reactions:
  - $2H_3O^+ + 2e^- \rightarrow 2H_2O + H_2$ (16)
  - $2H_2O + 2e^- \rightarrow 2OH^- + H_2$ (17)
  - $2H_2CO_3 + 2e^- \rightarrow 2HCO_3^- + H_2$ (18)
  - $2HCO_3^- + 2e^- \rightarrow 2CO_3^{2-} + H_2$ (19)
  - $2MDEAH^+ + 2e^- \rightarrow 2MDEA + H_2$ (20)

Since MDEA/CO_2/H_2O solution under the absorber condition is alkaline (close to pH 9), it can be shown that the contributions of H_3O^+ reduction and H_2CO_3 reduction reactions are quite small due to the very low concentrations in solution, when compared to other species. In addition, H_2O reduction kinetics is very slow and thus it was not considered in the present corrosion model. Thus, only HCO_3^- and $MDEAH^+$ reduction reactions (19 and 20) were considered as the key cathodic reactions in this system.

The rates of the electrochemical reactions at the steel surface depend on the electrical potential of the surface, the surface concentrations of species involved in the reactions and temperature. Since electrochemical reactions involve exchange of electrons, the reaction rate can be conveniently expressed as a rate at which the electrons are "consumed or released" (i.e., in terms of an electrical current density, i). Fundamental rate equations of electrochemistry relate i to the potential at the steel surface (E), via an exponential relationship:[18]

$$i = i_o \times 10^{\pm \frac{E - E_{rev}}{b}} \quad (21)$$

which can be written down for each of the electrochemical reactions involved in the corrosion process. The positive sign applies for the anodic reaction while the negative sign applies for the cathodic reactions. i_o is the exchange current density, E_{rev} is the reversible potential and b is the Tafel slope. In most cases, i_o and E_{rev} are nonlinear functions of the surface concentration of species involved in a particular reaction, while all three parameters are functions of temperature.

Implementation of the model

The model requires as input: pH, HCO_3^- concentration, and $MDEAH^+$ concentration. Once the input parameters are determined, the model calculates individual and total cathodic and anodic currents (rates). At the balance of the total cathodic and anodic currents (rates) one can find corrosion potential (E_{corr}) by solving:

$$i_{Fe} = i_{HCO_3^-} + i_{MDEAH^+} \quad (22)$$

Corrosion current density (i_{corr}) is calculated from the anodic reaction current (i_{Fe}) and the known E_{corr}. Finally the corrosion rate is then recovered by using Faraday's law. If the unit A/m^2 is used for the corrosion current density, then conveniently the corrosion rate for carbon steel expressed in mm/y takes almost the same numerical value, precisely: $CR = 1.155 \times i_{corr}$.

Verification: Comparison with experiments

The specimens made of carbon steel (ASTM[(1)] A36) with a chemical composition of 0.23% C, 0.79% Mn, 0.02% P, 0.03% S, 0.29% Cu, 0.20% Si, and balance Fe. The specimens were ground with 600-grit silicon carbide (SiC) paper, cleaned with isopropyl alcohol (C_3H_8O) in an ultrasonic bath, and dried prior to exposure. An aqueous solution of MDEA with a concentration of 50% by weight was prepared from a 99% pure MDEA reagent and deionized (DI) water. The test solution was purged with 12% CO_2 gas (pCO_2=0.12 bar: CO_2 loading= 0.13 mol CO_2/mol amine).

Corrosion tests were carried out in a 2-L glass cell at 50°C under atmospheric pressure. Further details of the experimental setup can be found elsewhere.[19]

RESULTS

Speciation model for an MDEA/CO_2/H_2O system

Figure 2 shows the activity (which is defined as the activity coefficient (γ_i) times concentration (c_i)) for the species in a 50 wt.% MDEA system at 50°C at different CO_2 partial pressures. As shown in Figure 2, activities of MDEA and CO_3^{2-} decreased with CO_2 partial pressure whereas they increased for $MDEAH^+$, and HCO_3^-.

The calculated pH of 50 wt.% MDEA solution at 50°C under different CO_2 partial pressures is compared with the measurements in Figure 3. The comparison of the calculated CO_2 loading as a function of partial pressure of CO_2 with our own and open literature[20] data is shown in the same figure. There it can be seen that the speciation model performs reasonably well.

([1]) American Society for Testing Materials (ASTM) International, 100 Barr Harbor Dr., West Conshohocken, PA 19428.

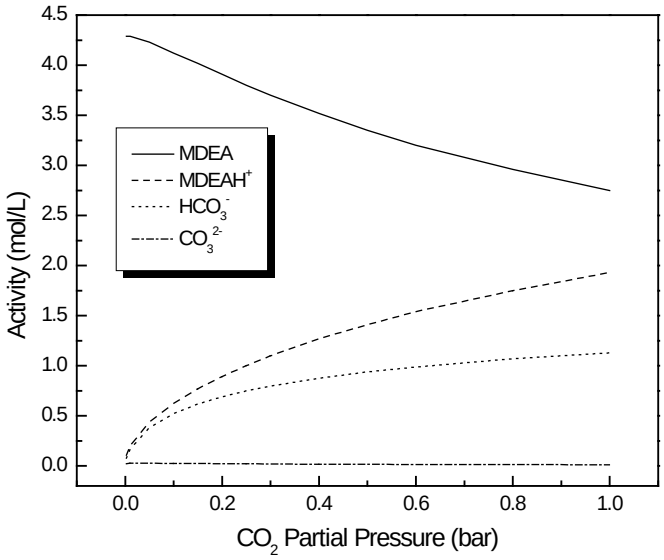

Figure 2: Activity of species in 50% MDEA system at 50°C as a function of partial pressure of CO_2

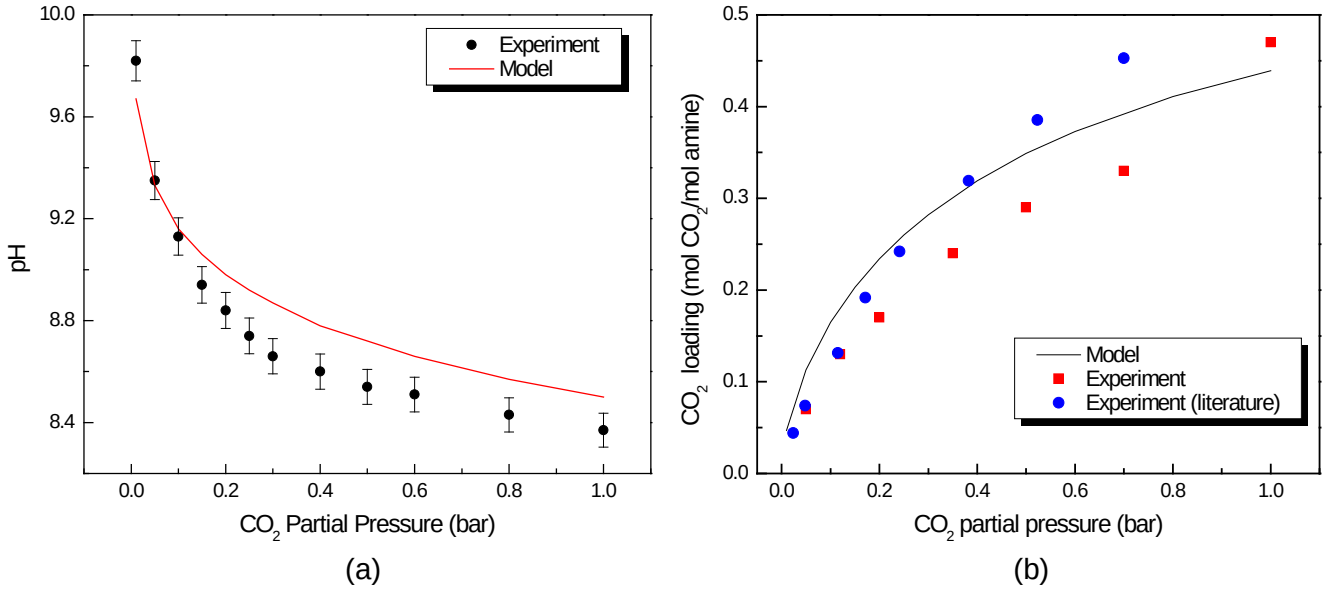

Figure 3: Comparison between experimental data and calculations; (a) pH and (b) CO_2 loading at different CO_2 partial pressures (50% MDEA system at 50°C).

Corrosion of carbon steel in an MDEA/CO_2/H_2O system

The electrochemical parameters for the reactions which were considered in the present study are summarized in Table 1 and Table 2. They were found in the open literature,[18,21] and determined from the electrochemical data obtained in the present study.

Table 1
Electrochemical Parameters for the Exchange Current Density Included in the Model

	i_o (A/m^2)	$i_{o,ref}$ (A/m^2)	$c_{H^+,ref}$ (molar)	$c_{HCO_3^-,ref}$ (molar)	$c_{MDEAH^+,ref}$ (molar)
Fe oxidation (15)	$i_{o,Fe} = i_{o,Fe,ref}\left(\frac{c_{HCO_3^-}}{c_{HCO_3^-,ref}}\right)^{\alpha}\left(\frac{c_{H^+}}{c_{H^+,ref}}\right)^{\beta}$	0.53	$10^{-9.1}$	1	-
HCO_3^- reduction (19)	$i_{o,HCO_3^-} = i_{o,HCO_3^-,ref}\left(\frac{c_{HCO_3^-}}{c_{HCO_3^-,ref}}\right)^{\delta}$	0.15	-	0.5	-
$MDEAH^+$ reduction (20)	$i_{o,MDEAH^+} = i_{o,MDEAH^+,ref}\left(\frac{c_{MDEAH^+}}{c_{MDEAH^+,ref}}\right)^{\kappa}$	0.15	-	-	0.63

Table 2
Electrochemical Parameters for the Reversible Potential and Tafel Slope Included in the Model

	E_{rev} (V)	b (V)
Fe oxidation (15)	$E_{rev} = E_{o,Fe^{2+}/Fe} + \frac{2.3RT}{2F}\log c_{Fe^{2+}}$	0.12
HCO_3^- reduction (19)	$E_{rev} = -\frac{2.3RT}{F}pH$	$b = \frac{2.3RT}{0.5F}$
$MDEAH^+$ reduction (20)	$E_{rev} = -\frac{2.3RT}{F}pH$	$b = \frac{2.3RT}{0.5F}$

Determination of reaction order

Iron dissolution: In order to determine reaction orders with respect to HCO_3^- and H^+ for iron dissolution reaction, polarization tests were conducted under different test conditions shown in Table 3.

Figure 4 shows the anodic polarization curves of carbon steel at different HCO_3^- concentrations. It can be clearly seen that anodic current density increased and corrosion potential decreased with increasing HCO_3^- concentration. Figure 5 is a plot of the log of the current density at constant potential (-0.74 V) versus the log of the concentration of HCO_3^- at pH 9.1. The slope is 1.86, indicating that the reaction order (α) is close to 2. Figure 6 shows the measured anodic polarization curves and the calculated Tafel lines at different HCO_3^- concentrations. The Tafel lines were produced with the reaction order of 2 and the Tafel slope of 0.12 V/dec. A reasonable agreement is seen, considering that there is very little linearity in the measured curves, which is likely due to passivation of the steel surface caused by polarization.

Figure 7 shows the anodic polarization curves of carbon steel at different pH values. The anodic current density increased and the corrosion potential decreased with increasing pH. Figure 8 is a plot of the log of the current density at constant potential (-0.7 V) versus the log of the pH. The slope of the plot showed a slope of approximately -0.5, indicating that the reaction order (β). Figure 9 shows the measured anodic polarization curves and the calculated Tafel lines at different pH. The Tafel lines were produced with the reaction order of -0.5 and the Tafel slope of 0.12 V/dec. Again the agreement can be considered being reasonable considering the nonlinearity of the experimental curves due to passivation.

Based on the results presented above, reaction orders of HCO_3^- and H^+ for iron dissolution reaction were determined as:

$$i_{o,Fe} = i_{o,Fe,ref}\left(\frac{c_{HCO_3^-}}{c_{HCO_3^-,ref}}\right)^2\left(\frac{c_{H^+}}{c_{H^+,ref}}\right)^{-0.5} \quad (23)$$

Table 3
Test Conditions for Determining Iron Dissolution Reaction Orders

	Solutions	HCO_3^- concentration (mol/L)	pH	Temperature (^oC)
α	$NaHCO_3/Na_2CO_3/H_2O$	0.5, 1.0, 1.5	9.1	50
β	$NaHCO_3/Na_2CO_3/H_2O$	1.0	7, 8, 9	50

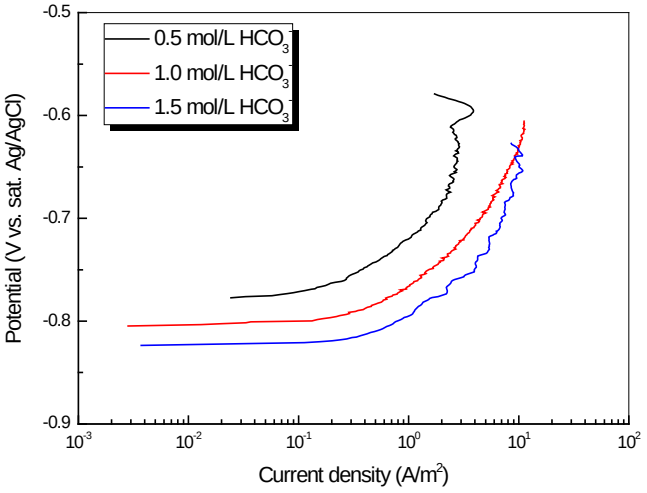

Figure 4: Anodic polarization curves for carbon steel at different HCO_3^- concentrations.

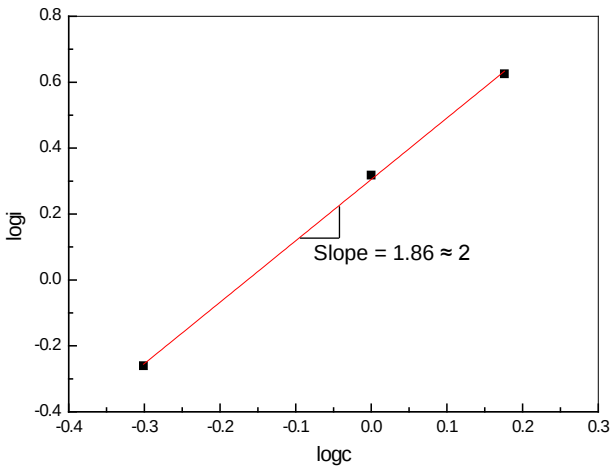

Figure 5: Determination of iron dissolution reaction order wrt HCO_3^- concentration.

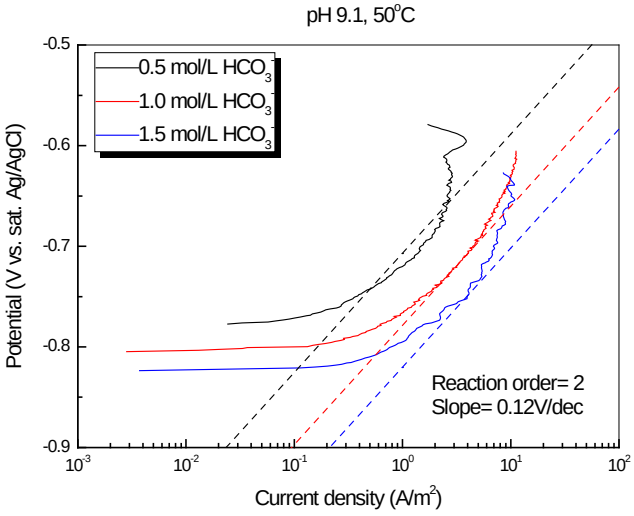

Figure 6: Measured anodic polarization curve and calculated Tafel lines for iron dissolution at different HCO_3^- concentrations.

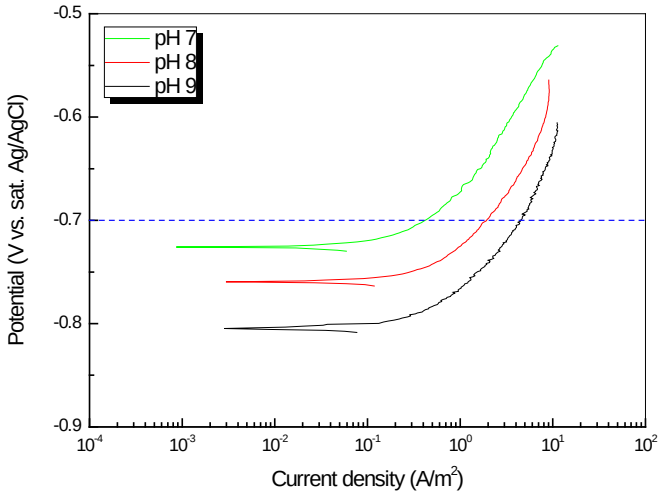

Figure 7: Anodic polarization curves of carbon steel at different pH.

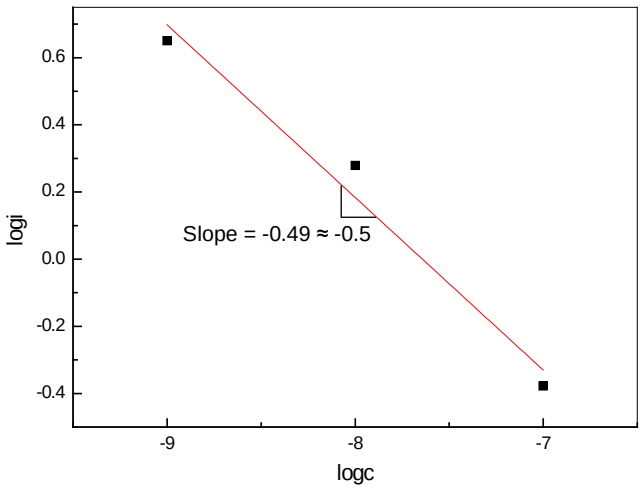

Figure 8: Determination of the iron dissolution reaction order wrt H^+ concentration.

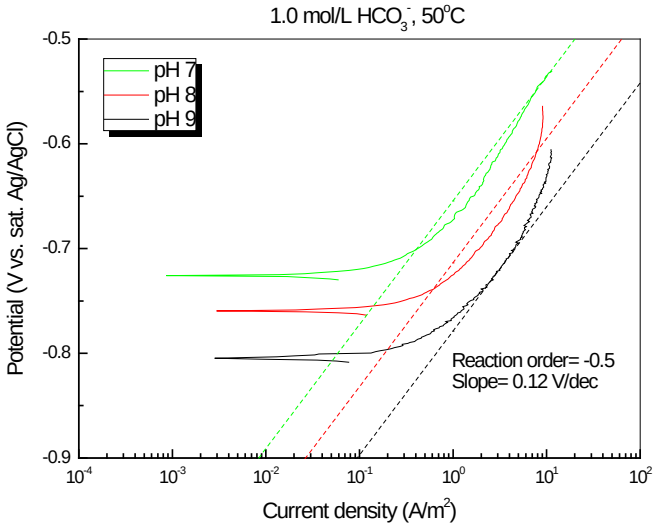

Figure 9: Measured anodic polarization curves and calculated iron Tafel lines for dissolution at different pH.

Bicarbonate reduction: In order to determine the reaction order for the HCO_3^- reduction reaction (19), cathodic polarization tests were conducted using a range of test conditions as shown in Table 4.

Figure 10 shows the cathodic polarization curves of carbon steel at different HCO_3^- concentrations at pH 9.1. The cathodic current density slightly increased and the corrosion potential decreased with increasing HCO_3^- concentration. Figure 11 is a plot of the log of the current density at constant potential (-0.95 V) versus the log of the concentration of HCO_3^-. The slope of the line in the plot is 0.39, indicating that the reaction order (δ) is close to 0.5. Figure 12 shows the measured cathodic polarization curves and the calculated Tafel lines at different HCO_3^- concentrations. The Tafel lines were produced with the reaction order of 0.5 and the Tafel slope of 0.128 V/dec. A reasonable agreement between experimental polarization curves and calculated Tafel lines is seen, although one can argue that this effect is within the margins of experimental error. Based on these result, the reaction order for HCO_3^- reduction reaction was determined as:

$$i_{o,HCO_3^-} = i_{o,HCO_3^-,ref}\left(\frac{c_{HCO_3^-}}{c_{HCO_3^-,ref}}\right)^{0.5} \quad (24)$$

Table 4
Test Conditions for Determining the HCO_3^- Reduction Reaction Order

	Solutions	HCO_3^- concentration (mol/L)	pH	Temperature (^oC)
δ	$NaHCO_3/Na_2CO_3/H_2O$	0.5, 1.0, 1.5	9.1	50

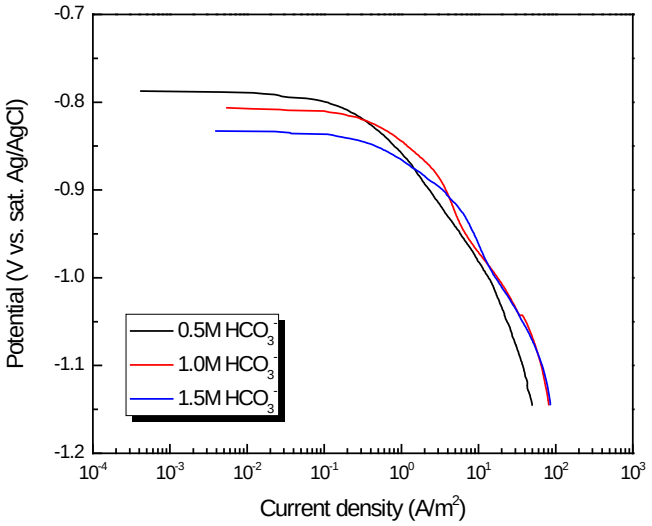

Figure 10: Cathodic polarization curves for carbon steel at different HCO_3^- concentrations.

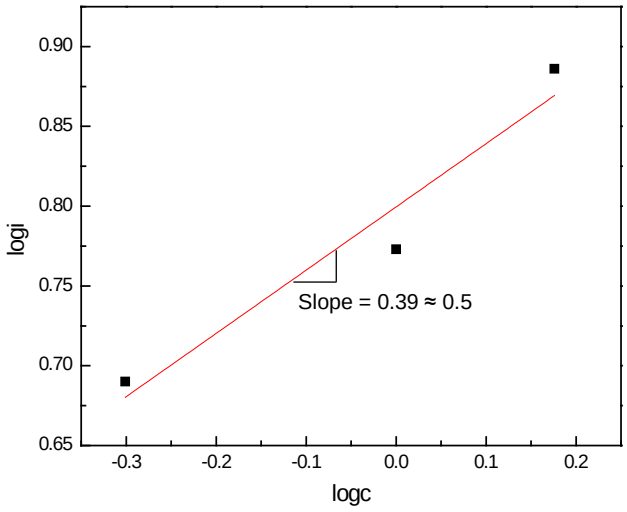

Figure 11: Determination of the reaction order for HCO_3^- reduction.

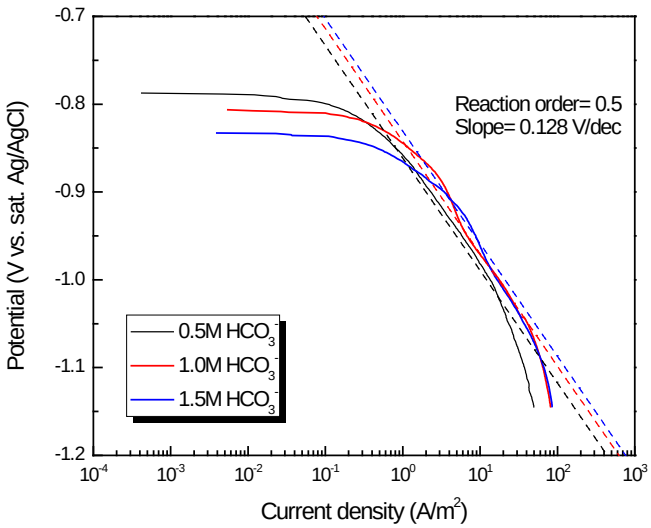

Figure 12: Measured cathodic polarization curve and calculated Tafel lines for HCO_3^- reduction at different HCO_3^- concentrations.

Protonated MDEA reduction: In order to determine the reaction order for the $MDEAH^+$ reduction reaction (20), cathodic polarization tests were conducted at different test conditions shown in Table 5.

Figure 13 shows the cathodic polarization curves for carbon steel at different $MDEAH^+$ concentrations at pH 9.1. The cathodic current density increased with increasing $MDEAH^+$ concentration. Figure 14 is a plot of the log of the current density at constant potential (-0.8 V) versus the log of the concentration of $MDEA^+$. The slope of the line in the plot is approximately 1.3, indicating that the reaction order (κ) is close to 1. Figure 15 shows the comparison of the measured cathodic polarization curves and the calculated Tafel lines at different $MDEAH^+$ concentrations. The Tafel lines were produced with the reaction order of 1 and the Tafel slope of 0.128 V/dec. A good agreement between experimental polarization curve and calculated Tafel line at different $MDEAH^+$ concentrations is seen.

Based on these result, a reaction order for $MDEAH^+$ reduction reaction was determined as:

$$i_{o,MDEAH^+} = i_{o,MDEAH^+,ref}\left(\frac{c_{MDEAH^+}}{c_{MDEAH^+,ref}}\right)^1 \quad (25)$$

Table 5
Test Conditions for Determining the Reaction Order for $MDEAH^+$ Reduction

	Solutions	$MDEAH^+$ concentration (mol/L)	pH	Temperature (^oC)
κ	$MDEA/HCl/H_2O$	0.33, 0.63, 1	9.1	50

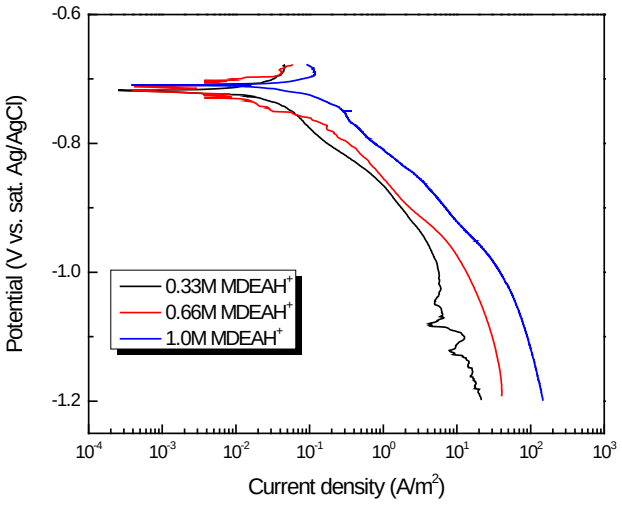

Figure 13: Cathodic polarization curves for carbon steel at different $MDEAH^+$ concentrations.

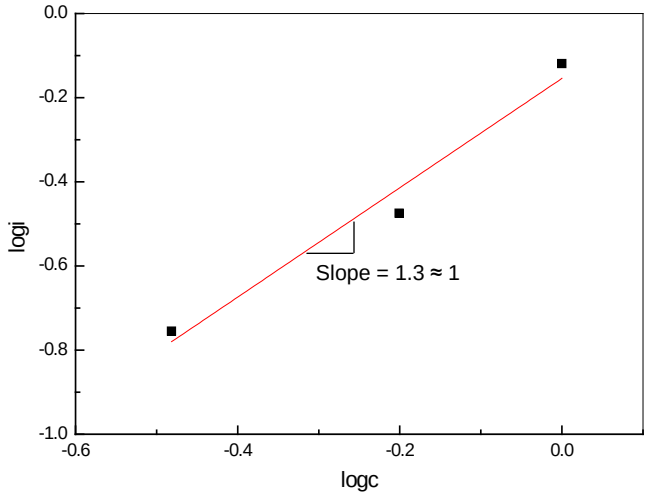

Figure 14: Determination of the reaction order for $MDEAH^+$ reduction.

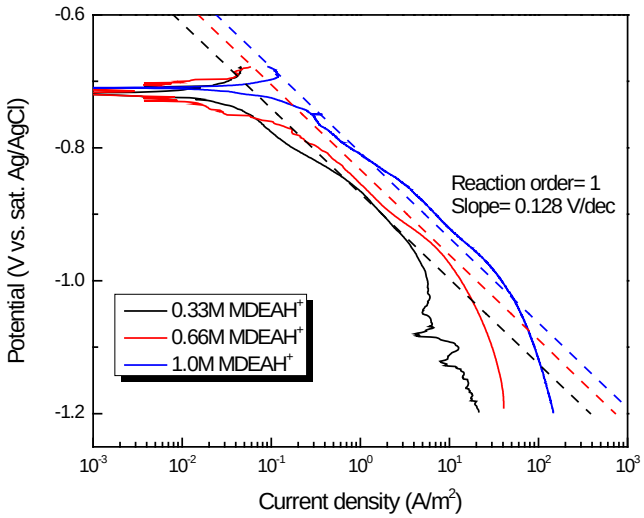

Figure 15: Measured cathodic polarization curves and calculated Tafel lines for $MDEAH^+$ reduction at different $MDEAH^+$ concentrations

Validation of the overall corrosion model

Performance of the overall corrosion model was validated by comparing the predictions with results from experiments. Figure 16 compares corrosion rates between experiment and prediction at different HCO_3^- concentrations and pH. The predicted corrosion rates showed good agreement with experimental data with an error not larger than 20-30%, which can be considered to be within the experiential error range for the current LPR measurements.

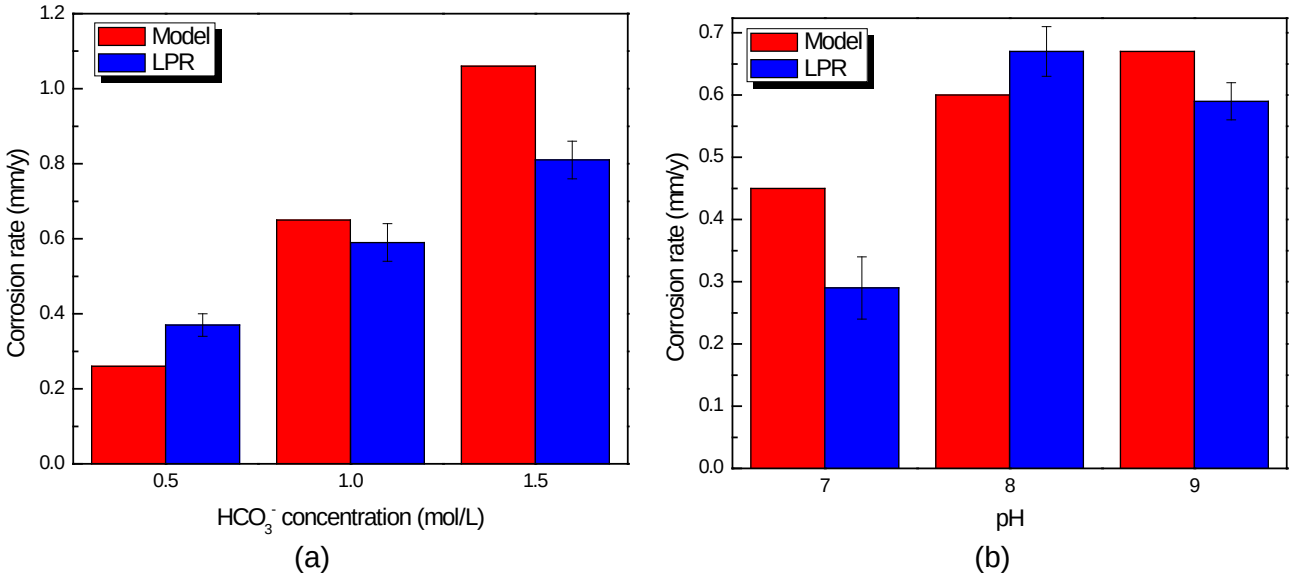

Figure 16: Comparison of corrosion rates between experiments and predictions at different conditions: (a) at different HCO_3^- concentrations (b) at different pH

Figure 17 shows the comparison of experimental and calculated polarization curves[19] and corrosion rates for a 50 wt.% MDEA / 12% CO_2 condition. Although predicted polarization curves indicate a higher corrosion potential than seen in the experiments, given the complexity of the system one can accept this result, particularly in the light of the reasonable agreement of the corrosion current / rate, as indicated in the same figure. Many similar comparisons were made for other conditions covered in this study – with similar results. This indicates that the current corrosion model is applicable to uniform

corrosion of carbon steel in the absorber conditions, as long as there is no major deviation from the conditions studied here: MDEA concentration (50 wt.%) and temperature (50°C). Further work is ongoing in order to extend the validity of the model to cover a broader range of conditions such as those seen in the regenerator.

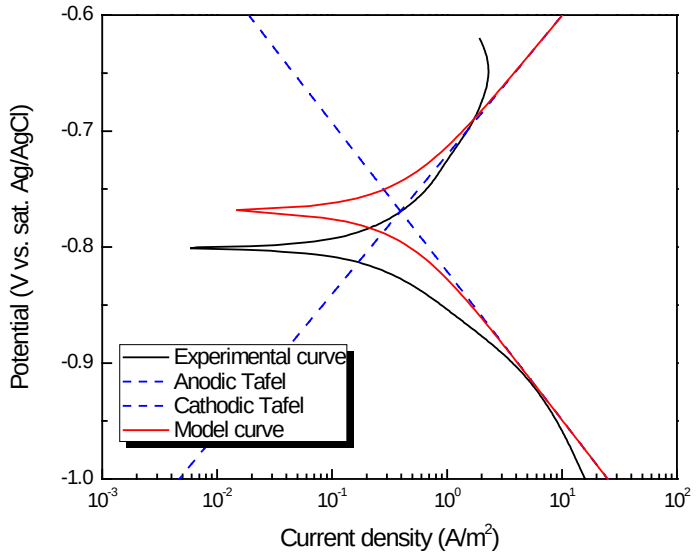

(a)

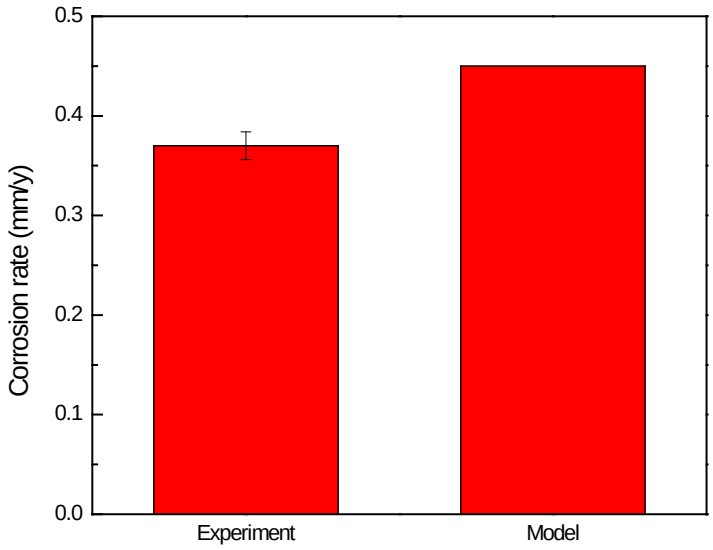

(b)

Figure 17: Comparison between experimental data and predictions in a 50 wt.% MDEA/12% CO_2 system at 50°C: (a) polarization curves, (b) corrosion rates.

CONCLUSIONS

A predictive model was developed for corrosion of carbon steel in CO_2-loaded aqueous methyldiethanolamine (MDEA) systems based on modeling of solution speciation and electrochemical reactions. The following conclusions are drawn:

- Activities of MDEA and CO_3^{2-} decreased with CO_2 partial pressure whereas they increased with CO_2 partial pressure for $MDEAH^+$, and HCO_3^-.

- The speciation model showed a good agreement with experimental data for pH and CO_2 loading.
- The required electrochemical parameters (e.g., exchange current densities, Tafel slopes and reaction orders) for the Fe dissolution, HCO_3^- reduction and $MDEAH^+$ reduction reactions were determined by experiments, and used to successfully build a corrosion model for corrosion of carbon steel in MDEA/CO_2/H_2O environments.
- The corrosion model showed a good agreement with experimental data for various environmental conditions including pure CO_2 and MDEA/CO_2 solutions.

ACKNOWLEDGEMENTS

The authors would like to acknowledge the financial support from Alstom Power Inc. to the Institute for Corrosion and Multiphase Technology at Ohio University on this project.

REFERENCES

1. E. Fleury, J. Kittel, B. Vuillemin, R. Oltra, F. Ropital, "Corrosion in Amine Units for Acid Gas Treatment: A Laboratory Study," EUROCORR 2009, SS 12-O-7888 (Dechema e.V. 2009).

2. W. Tanthapanichakoon, A. Veawab, B. McGarvey, "Electrochemical Investigation on the Effect of Heat-stable Salts on Corrosion in CO_2 Capture Plants Using Aqueous Solution of MEA," *Ind. Eng. Chem. Res.* 45 (2006): p. 2586.

3. W. Liu, D. King, J. Liu, B. Johmson, Y. Wang, Z. Yang, "Critical Material and Process Issues for CO_2 Separation from Coal-Powered Plants," *JOM* 61 (2009): p. 36.

4. M.R. Khorrami, K. Raeissi, H. Shahban, M.A. Torkan, A. Saatchi, "Corrosion Behavior of Carbon Steel in Carbon Dioxide-Loaded Activated Methyl Diethanol Amine Solution," *Corrosion* 64 (2008): p. 124.

5. M.S. DuPart, T.R. Bacon, D.J. Edwards, "Understanding Corrosion in Alkanolamine Gas Treating Plants: Part 2," *Hydrocarb. Process.* (1993): p. 89.

6. Y. Tomoe, M. Shimizu, H. Kaneta, "Active Dissolution and Natural Passivation of Carbon Steel in Carbon Dioxide-Loaded Alkanolamine Solutions," CORROSION/96, paper no. 395 (Houston, TX: NACE International, 1996).

7. X.-P. Guo, Y. Tomoe, "The Effect of Corrosion Product Layers on the Anodic and Cathodic Reactions of Carbon Steel in CO_2-Saturated MDEA Solutions at 100^{o}C," *Corros. Sci.* 41 (1999): p. 1391.

8. A. Veawab, P. Tontiwachwuthikul, A. Chakma, "Corrosion Behavior of Carbon Steel in the CO_2 Absorption Process Using Aqueous Amine Solutions," *Ind. Eng. Chem. Res.* 38 (1999): p. 3917.

9. M. Nainar, A. Veawab, "Corrosion in CO_2 Capture Process Using Blended Monoethanolamine and Piperazine," *Ind. Eng. Chem. Res.* 48 (2009): p. 9299.

10. A. Veawab, P. Tontiwachwuthikul, A. Chakma, "Investigation of Low-Toxic Organic Corrosion Inhibitors for CO_2 Separation Process Using Aqueous MEA Solvent," *Ind. Eng. Chem. Res.* 40 (2001): p. 4771.

11. W. Tanthapanichakoon, A. Veawab, "Polarization Behavior and Performance of Inorganic Corrosion Inhibitors in Monoethanolamine Solution Containing Carbon Dioxide and Heat-Stable Salts," *Corrosion* 61 (2005): p. 371.

12. S. Rennie, “Corrosion and Materials Selection for Amine Service,” *Materials Forum* 30 (2006): p. 126.

13. A. Veawab, A. Aroonwilas, “Identification of Oxidizing Agents in Aqueous Amine-CO_2 Systems using a Mechanistic Corrosion Model,” *Corrosion Science* 44 (2002): p. 967.

14. A. Vrachnos, G. Kontogeorgis, E. Voutsas, “Thermodynamic Modeling of Acidic Gas Solubility in Aqueous Solutions of MEA, MDEA and MEA-MDEA Blends,” *Ind. Eng. Chem. Res.* 45 (2006): p. 5148.

15. H.A. Al-Ghawas, D.P. Hagewiesche, G. Ruiz-Ibanez, O.C. Sandall, “Physicochemical Properties Important for Carbon-Dioxide Absorption in Aqueous Methyldiethanolamine,” *J. Chem. Eng. Data* 34 (1989): p. 385.

16. A. Benamor, M.K. Aroua, “Modeling of CO_2 Solubility and Carbamate Concentration in DEA, MDEA and Their Mixtures using the Deshmukh-Mather Model,” *Fluid Phase Equilibria* 231 (2005): p. 150.

17. G.N. Lewis, *Thermodynamics*. Second ed. 1961, New York: McGRAW-HILL BOOKCOMPANY. 640.

18. M. Nordsveen, S. Nesic, R. Nyborg, A. Stangeland, “A Mechanistic Model for Carbon Dioxide Corrosion of Mild Steel in the Presence of Protective Iron Carbonate Films- Part 1: Theory and Verification,” *Corrosion* 59 (2003): p. 443.

19. Y.S. Choi, D. Duan, S. Nesic, F. Vitse, S.A. Bedell, C. Worley, “Effect of Oxygen and Heat Stable Salts on the Corrosion of Carbon Steel in MDEA-Based CO_2 Capture Process,” *Corrosion* 66 (2010): p. 125004.

20. M.K. Park, O.C. Sandall, “Solubility of Carbon Dioxide and Nitrous Oxide in 50 mass % Methyldiethanolamine,” *J. Chem. Eng. Data* 46 (2001): p. 166.

21. S. Nesic, J. Postlethwaite, S. Olsen, “An Electrochemical Model for Prediction of Corrosion of Mild Steel in Aqueous Carbon Dioxide Solutions,” *Corrosion* 52 (1996): p. 280.